Strain-Induced Formation of Surface Defects in Amorphous Silica: A Theoretical Prediction

Chin-Lung Kuo, Sangheon Lee, and Gyeong S. Hwang*

Department of Chemical Engineering, University of Texas, Austin, Texas 78713, USA

(Received 2 July 2007; published 21 February 2008)

We present a prediction for the formation of surface defects in a thin amorphous silica layer during relaxation of externally imposed stresses and strains, based on extensive *ab initio* molecular dynamics calculations. Our calculations show that the application of a biaxial compressive stress leads to the creation of edge-sharing tetrahedron and/or silanone defects at the silica surface, which turns out to facilitate strain relief with irreversible structural changes in the silica layer. We also discuss a possible correlation between the predicted formation of surface defects and the observed enhanced surface reactivity of amorphous silica under compressive strain conditions.

DOI: 10.1103/PhysRevLett.100.076104 PACS numbers: 68.35.−p, 61.72.J−, 68.47.Gh

While a defect-free silica surface is relatively inert, previous experiments [1–3] have evidenced that the surface reactivity can be enhanced in the presence of intrinsic stress. It has been thought that the enhanced reactivity of silica surfaces under strain conditions could be primarily attributed to the strain-induced bending of Si-O-Si linkages which would make inert Si-O bonds active. Indeed, a recent infrared spectroscopy experiment [2] showed a decrease in the average Si-O-Si bond angle from 144 to 141° with lowering the oxidation temperature from 1050 to 800 °C. However, it is hard to expect that only a 3° decrease in the Si-O-Si bond angle would cause a threefold increase in the number density of Si nanoparticles on the SiO_2 surface [2]. Earlier molecular orbital calculations [4] also showed that a substantial increase in the silica surface reactivity could be achieved with Si-O-Si angles only below 120°. While it is evident that a compressive stress leads to the creation of certain favorable nucleation sites for Si nanoparticle growth on the SiO_2 surface, the underlying reason still remains a subject of speculation.

In this Letter, we present changes in the surface structure and reactivity of thin amorphous silica films under biaxial compressive strain, based on extensive Monte Carlo and density functional theory calculations. We first constructed several defect-free thin amorphous SiO_2 (a-SiO_2) slabs using a combination of continuous random network model based METROPOLIS Monte Carlo (CRN-MMC) and *ab initio* molecular dynamics (MD) simulations. Then, we performed extensive *ab intio* MD simulations to examine possible structural changes in a thin a-SiO_2 slab upon biaxial compression. We find that the externally imposed strain can be lowered by creating edge-sharing tetrahedra and/or silanone groups at the surface of a-SiO_2, while the former is prevailing than the latter. The surface defect formation is considered as two-dimensional densification because it leads to the reduction of Si-O-Si linkages on the surface. This also turns out to assist in relieving the impose strain with irreversible structural changes in the SiO_2 slab. Our results also suggest that the surface reactivity enhancement of a-SiO_2 towards Si nanoparticle growth under compressive strain conditions could be attributed to the formation of surface defects, particularly edge-sharing tetrahedra (i.e., two-membered rings) given that the silanone defect hardly interacts with Si atoms.

In fact, the surface structure and function of oxide materials are commonly governed by pointlike surface defects [5]. It is, however, a challenging task to characterize and quantify experimentally stress-induced changes in the surface structure of oxide materials, which is largely due to the difficulty of direct measurement arising from sample charging. Nonetheless, earlier experiments evidenced the existence of edge-sharing tetrahedra on a dry a-SiO_2 surface after high temperature thermal treatment [6], based on well-defined infrared absorption bands at 888 and 908 cm^{-1} (similar to those of cyclodisiloxane molecules). In addition, as expected the highly strained two-membered rings have been found to be very active towards various surface reactions [7,8]. While the underlying formation mechanism of edge-sharing tetrahedra is still ambiguous, our first principles study shows the possibility that the surface defect can be formed by thermally activated structural relaxation under compressive strain. Silanone formation has also been proposed to account for the Si Auger peak at 91 eV on a heavily electron-irradiated SiO_2 surface [9]. The silanone defect was also often observed on a mechanically grinded or crushed surface [10]. In addition, transformation of O vacancy to silanone on a-SiO_2 was recently predicted based on density functional calculations [11]. While the previous studies showed silanone formation associated with O deficient centers, this work suggests another possible formation route driven by an internal or external stress.

In this work, for good statistics five different slab structures were employed to mimic the thin amorphous layer of SiO_2. Each slab is about 10 Å thick, while providing two defect-free surfaces. The model structures were constructed using CRN-MMC simulations. We began by placing 36 or 48 SiO_2 units in a given size of supercell which corresponds, respectively, to the $(2 \times 2 \times 1)$ or $(3 \times 2 \times 1)$ cell of ideal β-cristobalite with a lattice constant of 5.76 Å (the equilibrium lattice constant of ideal β-cristobalite is 7.42 Å). The top and bottom layer Si

 © 2008 The American Physical Society

atoms were all passivated with O atoms, yielding two defect-free surfaces. The highly strained initial structures were then relaxed via a sequence of bond transpositions using the METROPOLIS Monte Carlo sampling based on energetics from Keating-like potentials for silica [12]. During the relaxation, periodic boundary conditions were employed in both x and y directions while the z direction was released. The amorphous slab structures were further relaxed using *ab initio* MD at 1000 K for 1 ps within a Born-Oppenheimer framework, followed by static structural optimization. The optimized structures of amorphous SiO_2 slabs are free of coordination defects as well as edge-sharing tetrahedra. The computed strain energies of the five sample slab structures considered, relative to α-quartz, range from 0.49 to 0.59 eV per SiO_2 unit (see Table I).

All atomic structures and energies reported herein were calculated using the well-established plane-wave program VASP [13]. We used the generalized gradient approximation (GGA) derived by Perdew and Wang (PW91) [14]. A plane-wave basis set for valence electron states and Vanderbilt ultrasoft pseudopotentials for core-electron interactions were employed. A plane-wave cutoff energy of 300 eV was used for *ab initio* MD simulations and 400 eV for static calculations of structure and energetics. The Brillouin zone integration was performed using one k point (at Gamma). In the slab calculations, periodic boundary conditions were employed in all three directions with a vacuum gap of 12 Å in the z direction to separate two distinct surfaces. All atoms were relaxed using the conjugate gradient method until residual forces on constituent atoms become smaller than 5×10^{-2} eV/Å.

We first looked at how the strain energy of a thin a-SiO_2 slab changes with varying compressive biaxial strains. The biaxial compressive strain was introduced by reducing the lateral size of simulation cell in both x and y directions (as illustrated in the inset of Fig. 1). Here, no bond transposition is allowed. Thus, the energy variation mainly arises from strain-induced lattice distortions, associated with bond stretching, bond angle bending, torsion strain, and nonbonding interactions. As shown in Fig. 1, the elastic strain energy increases in a quadratic manner with increasing the compressive strain. Under 10% strain, the strain energy increase is about 0.4 eV per SiO_2 unit. We can also notice that there is no significant change in the O-Si-O bond angle in a tetrahedron while the Si-O-Si bond angle distribution is noticeably altered with the compressive strain. That is, the bond angles decrease from $136 \pm 14.3°$ and $109.4 \pm 7.4°$ to $129.0 \pm 15.7°$ and $109.1 \pm 10.4°$, respectively, upon the application of 10% biaxial strain. This is not surprising considering that the Si-O-Si linkage is more flexible and deformable than the O-Si-O bond.

TABLE I. Relative energies per SiO_2 unit (in eV) for five different slab structures employed (S1-S3: 36 SiO_2 units, S4-S5: 48 SiO_2 units), with respect to α quartz, under no strain and 10% compressive strain [before (BR) and after (AR) structural relaxation]. The numbers of edge-sharing tetrahedra (ET) and silanone groups (SG) created during the structural relaxation under 10% compressive strain are also indicated.

	S1	S2	S3	S4	S5
No strain	0.59	0.53	0.52	0.49	0.58
10% (BR)	0.99	0.95	0.88	0.91	0.97
10% (AR)	0.71	0.58	0.68	0.61	0.63
ET/SG	2/0	2/1	0/2	2/1	2/1

Next, using *ab initio* MD simulations we examined changes in the structure of a thin a-SiO_2 slab, such as O-Si-O and Si-O-Si bond angle distributions, under biaxial compression. Under 10% strain, there are significant bond rearrangements that lead to irreversible changes in the a-SiO_2 layer structure. After the structural relaxation, as shown in Fig. 2 a small peak appears in between 85° and 90° in the Si-O-Si bond angle distribution while the tetrahedral O-Si-O bond angles remain almost unchanged. We find that the small peak originates from edge-sharing tetrahedra which are all located on the a-SiO_2 slab surfaces. It is also important to note that if the small peak is excluded the average value of the Si-O-Si bond angle distribution in the remaining part is 136.4° with the standard deviation of 16.0°, very close to 136.5° ± 14.8° as obtained under no external strain. We also find that the structural relaxation leads to creation of silanone groups on the amorphous surface. To assure the strain-induced formation of surface defects, we examined five different a-SiO_2 slabs under 10% compressive stain, yielding consistently edge-sharing tetrahedra and silanone groups (see Table I). This demon-

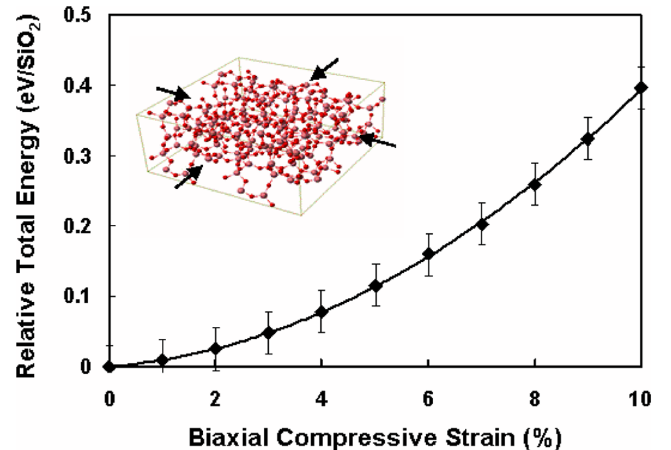

FIG. 1 (color online). Variation in the relative total energy per O-Si-O unit of a thin amorphous SiO_2 slab employed as a function of biaxial compressive strain (at %), as illustrated in the inset. In the inset, the small dark (red) and the large gray (pink) balls indicate O and Si atoms, respectively, and the arrows represent the direction of strain imposed on the a-SiO_2 slab. The computed average values (filled symbols) are well fitted into a quadratic curve (solid line), $y \approx 0.033x^2 + 0.0061x$, where y and x are the relative energy and the strain at %. The linear term arises from the existence of intrinsic in-plane stresses in the finite a-SiO_2 slabs employed.

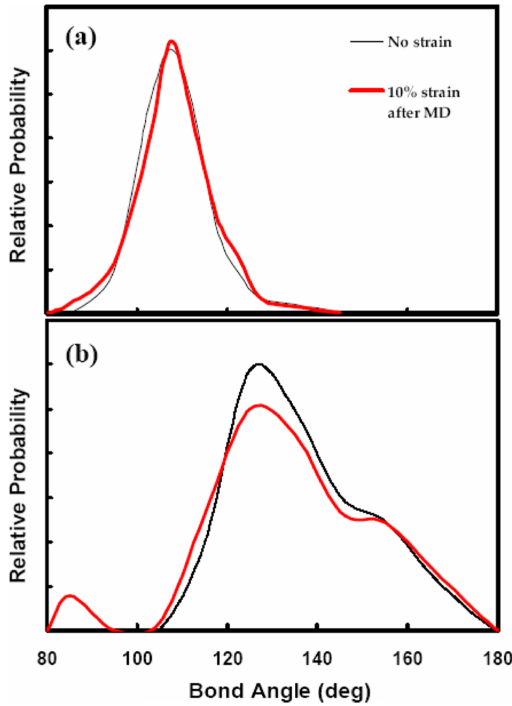

FIG. 2 (color online). Changes in the (a) O-Si-O and (b) Si-O-Si bond angle distributions under biaxial compressive strain. The thin (black) and thick (red) lines represent the bond angle distributions before and after imposing a compressive strain of 10%, respectively, as indicated. Here, the strained slab structure was relaxed using *ab initio* MD at 1200 K for 15 ps.

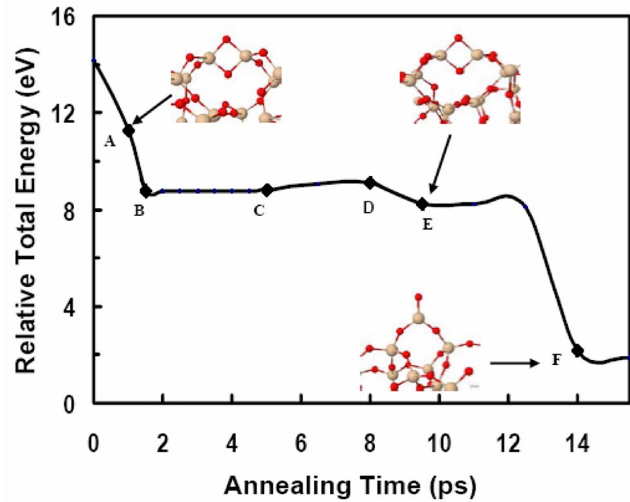

FIG. 3 (color online). Variation in the relative total energy (in eV) of a thin a-SiO_2 slab during *ab initio* MD relaxation at 1200 K as a function of annealing time (in ps). The strain-induced formation of surface edge-sharing tetrahedron and silanone defects is also indicated, together with their configurations (in the insets).

strates a strong correlation between the relief of externally imposed strain and the formation of surface defects.

Figure 3 illustrates how the total energy of a highly strained thin a-SiO_2 slab changes associated with formation of edge-sharing tetrahedra and/or silanone groups during the structural relaxation. Under 10% biaxial compression, our *ab initio* MD simulation at 1200 K shows that the initial structural relaxation through bond swaps takes place rapidly, thereby significantly lowering the slab strain energy within 1.5 ps. An edge-sharing tetrahedron forms around 1 ps (indicated as A). In between 1.5 and 5.0 ps (from B to C), no noticeable bond rearrangement occurs, and thus the total energy remains nearly unchanged. Then, the total energy slowly rises until another edge-sharing tetrahedron forms at 9.5 ps (E), via a saddle point (D) by overcoming a barrier of 0.3 eV. This is the only structural change observed between 5.0 and 9.5 ps. The energy gain from the second edge-sharing tetrahedron formation is estimated to be 0.6 eV. Although the edge-sharing linkage leads to highly strained siloxane bridges, the rest of the a-SiO_2 slab is likely to be relaxed enough to lower the total energy substantially. Figure 3 also shows a significant drop in the total energy between 11 and 15 ps. We find that this is mainly attributed to formation of a silanone group on the surface around 14 ps (E), accompanied with a series of bond rearrangements in the subsurface region. Our MD simulations also show that these two defect formation processes compete with each other, and are largely determined by the local bonding environment.

Figure 4 illustrates viable paths for the formation of an edge-sharing tetrahedron [(a)] and a silanone [(b)] on the a-SiO_2 surface under biaxial compression. As shown in Fig. 4(a), the edge-sharing tetrahedron formation is likely to be initiated by the electrostatic interaction of the positive Si atom at the SiO_4 tetrahedron's center (indicated as B) with a neighboring negative O atom (C). This may bring about an additional Si-O bonding interaction (D–E), followed by the rupture of two original Si-O bonds (B-D and C–E). Similarly, as illustrated in Fig. 4(b), the silanone formation is also initiated by the Si-O electrostatic interaction (A–C), yielding a threefold coordinated O (C) and fivefold coordinated Si (A) pair. This process then involves two successive Si-O bond breakages (B–C and A–D) to annihilate the coordination defect pair, resulting in a silanone group. The surface defect formation can be considered as two-dimensional densification, as it leads to a reduction in the number of O-Si-O linkages on the surface. Although the surface compressive strain appears to be more effectively relieved via silanone formation, the number density of edge-sharing tetrahedra is about twice greater than that of silanone defects. This is not surprising considering that the energy gain by strain relief over the energy loss by silanone defect formation is expected to be smaller than the case of edge-sharing tetrahedron creation.

In addition to defect formation, we also find that the structural relaxation leads to an increase in the average ring size of amorphous SiO_2 slabs. Before a strain is imposed, five and six-membered rings are prevailing, and three- and eight-membered rings are found to be the smallest and the largest ones, respectively, in five different model SiO_2 slab

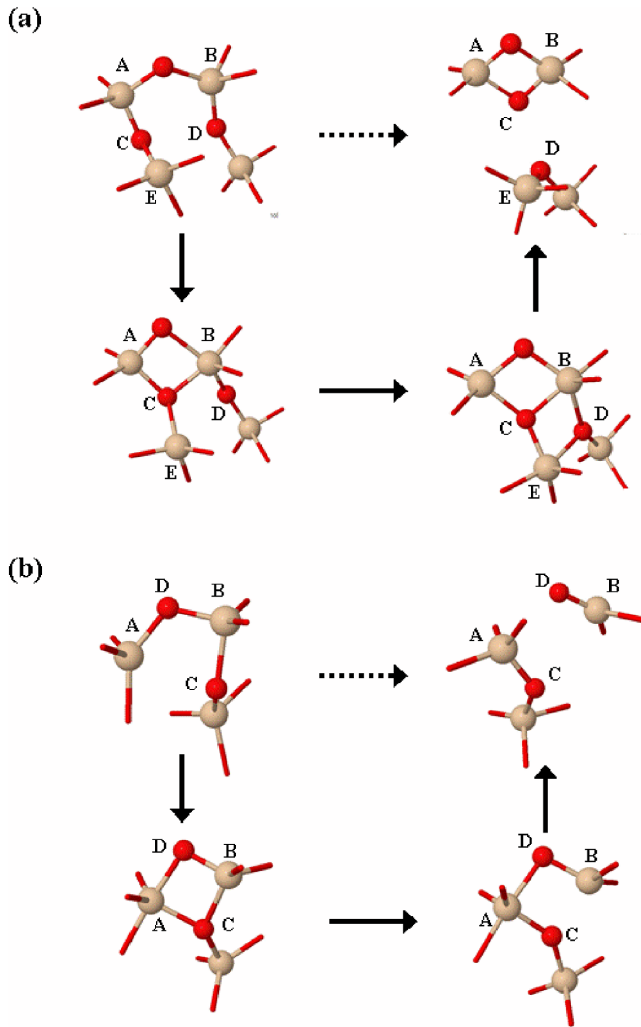

FIG. 4 (color online). Predicted viable routes for formation of (a) an edge-sharing tetrahedron and (b) a silanone group on the a-SiO_2 surface. The small dark (red) and large gray (pink) balls represent O and Si atoms, respectively.

structures examined. After structural relaxation under 10% strain, while five- and six-membered rings remain predominant, the ring-size distribution become broader due to formation of two- and nine-membered rings. In addition, the number of seven- and eight-membered rings is found to increase at the expense of three- to six-membered rings. As a result, the average ring size increases while the total number of rings reduces by about 5%. This is consistent with previous studies [15,16] predicting irreversible structural changes of amorphous SiO_2 which yield larger membered rings under compressive strain conditions. Our results also show that the irreversible structural change with larger size rings can be facilitated by the surface defect formation.

For the sake of comparison, finally we looked at possible structural changes in the thin a-SiO_2 slab under 5% strain. Note that under 5% strain the increase of strain energy is only one quarter of the case of 10% strain introduction. As also indicated by the small change in O-Si-O and Si-O-Si bond angle distributions the strain-induced structure deformation is insignificant. After *ab initio* MD annealing at 1300 K for 20 ps, no structural transformation is observed. Upon removing the external stress, the silica structure is completely restored. This suggests that when an externally imposed strain is insignificant the strain-induced structural change can be elastic and reversible with no appreciable bond defect formation and ring-size distribution change.

In conclusion, our study shows the possibility of tailoring the formation of surface defects in amorphous silica via external stress application. Given that surface defects commonly serve as active sites for various reactions on an oxide surface, this finding may provide a hint on how to manipulate the surface reactivity of amorphous silica by engineering strain-induced surface defects with existing experimental techniques.

We acknowledge National Science Foundation (No. CAREER-CTS-0449373) and Robert A. Welch Foundation (No. F-1535) for their financial support. We would also like to thank the Texas Advanced Computing Center for use of their computing resources.

*To whom correspondence should be addressed.
gshwang@che.utexas.edu

[1] S. Miyazaki, Y. Hamamoto, E. Yoshida, M. Ikeda, and M. Hirose, Thin Solid Films **369**, 55 (2000).
[2] F. Mazen, T. Baron, G. Brémond, N. Buffet, N. Rochat, P. Mur, and M. N. Séméria, J. Electrochem. Soc. **150**, G203 (2003).
[3] T. Baron, F. Mazen, C. Busseret, A. Souifi, P. Mur, F. Fournel, M. N. Séméria, H. Moriceau, B. Aspard, P. Gentile, and N. Magnea, Microelectron. Eng. **61–62**, 511 (2002).
[4] T. A. Michalske and B. C. Bunker, J. Appl. Phys. **56**, 2686 (1984).
[5] G. Pacchioni, L. Skuja, and L. D. Griscom, *Defects in* SiO_2 *and Related Dielectrics: Science and Technology* (Kluwer Academic, Dordrecht, Netherlands, 2000).
[6] C.-M. Chiang, B. R. Zegarski, and L. H. Dubois, J. Phys. Chem. **97**, 6948 (1993).
[7] A. Grabbe, T. A. Michalske, and W. L. Smith, J. Phys. Chem. **99**, 4648 (1995).
[8] L. H. Dubois and B. R. Zegarski, J. Am. Chem. Soc. **115**, 1190 (1993).
[9] V. M. Bermudez and V. H. Ritz, Phys. Rev. B **20**, 3446 (1979).
[10] V. A. Radtsig, Kinet. Catal. **40**, 693 (1999).
[11] C.-L. Kuo and G. S. Hwang, Phys. Rev. Lett. **97**, 066101 (2006).
[12] D. Yu, G. S. Hwang, T. A. Kirichenko, and S. K. Banerjee, Phys. Rev. B **72**, 205204 (2005), references cited therein.
[13] G. Kresse and J. Furthmuller, *VASP the Guide* (Vienna University of Technology, 2001).
[14] J. P. Perdew and Y. Wang, Phys. Rev. B **45**, 13 244 (1992).
[15] K. Trachenko and M. T. Dove, Phys. Rev. B **67**, 064107 (2003).
[16] L. Huang and J. Kieffer, Phys. Rev. B **69**, 224204 (2004).